

Quantitative error analysis of Discontinuous Galerkin methods for Linear Convection Equation

CHEN Qifan

Summer Research Project at The Ohio State Univeristy

My email:chanqifan@qq.com

Mentor: Y. Xing

YMC,2020

1 Introduction

- Discontinuous Galerkin method
- Fourier stability analysis

2 Error analysis with eigen-structures

- The case of P^1
- The case of P^2
- Nonuniform mesh

3 Implement to Fu's scheme

4 Conclusion and future work

Linear Convection Equation

Linear Convection Equation with periodic boundary conditions

$$\begin{aligned}u_t + u_x &= 0, x \in [0, 2\pi], t > 0 \\ u(x, 0) &= \sin x\end{aligned}$$

- Propagation of a wave without change of shape
- Most accessible equation in Computational Fluid Dynamics.
- Exact solution is $u(x, t) = \sin(x - t)$

Examples for Linear Convection Equation

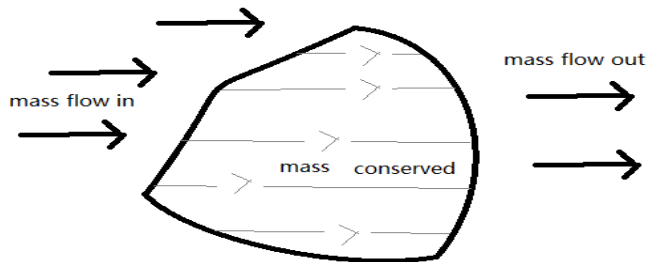
Conserved quantity: T with units of [stuff m^{-3}] :

Conservation equation:

$$\frac{\partial T}{\partial t} + \nabla \cdot \mathbf{F}_T = 0$$

where \mathbf{F}_T is the vector flux of T . Flux is velocity \times quantity: $\mathbf{F}_T = \mathbf{u}T$
with units [stuff m/s]

In one-dimension: $\frac{\partial T}{\partial t} + \frac{\partial uT}{\partial x} = 0$



Numerical Solution to PDE

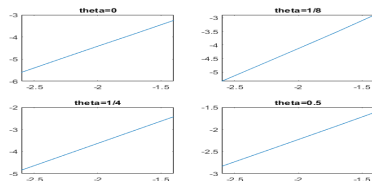


Figure: Order of accuracy: $\|u_{\text{numerical}} - u_{\text{exact}}\| = O(h^n)$

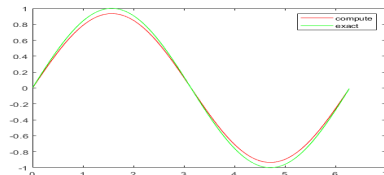


Figure: Structure Preserving: Energy conserving

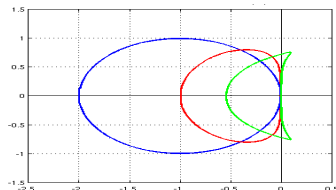


Figure: Stability region

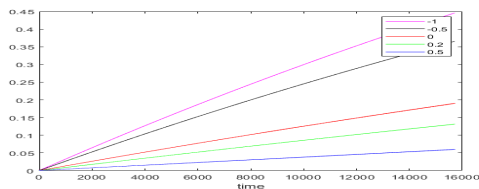


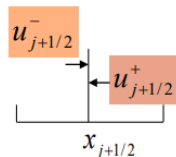
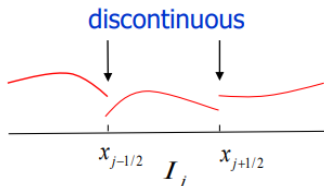
Figure: Exact error: coefficient on power function

Discontinuous Galerkin method

Solve PDE numerically: Finite difference, Finite volume, etc....

Finite element \rightarrow **Discontinuous Galerkin method**

- $I_h = \{I_j\}_{j=1}^N$: uniform partition of the computational domain $[0, 2\pi]$ into N cells : $0 = x_1 < x_{\frac{3}{2}} < \dots < x_{N+\frac{1}{2}} = 2\pi$. $\Delta x = \frac{2\pi}{N}$.
- Approximation space: $V_h^k = \left\{ v : v|_{I_j} \in P^k(I_j); 1 \leq j \leq N \right\}$
 $P^k(I_j)$: polynomials of degree up to k defined on the cell I_j .
- Local basis of $P^k(I_j)$: Lagrangian polynomials on the $k+1$ equally spaced points $x_{j+\frac{2l-k}{2(k+1)}} = x_j + \left(\frac{2l-k}{2(k+1)} \right) \Delta x$, $l = 0, \dots, k$



DG (semi-discrete) scheme

$$\int_{I_j} u_t v dx - \int_{I_j} u v_x dx + \hat{u}_{j+1/2} v_{j+1/2}^- - \hat{u}_{j-1/2} v_{j-1/2}^+ = 0$$

$\hat{u}_{j\pm\frac{1}{2}}$ is the numerical flux, v is the test function in V_h^k .

In this section, flux is chosen to be :

$$\hat{u}_{j\pm\frac{1}{2}} = u_{j\pm\frac{1}{2}}^- + \theta \left(u_{j\pm\frac{1}{2}}^+ - u_{j\pm\frac{1}{2}}^- \right), \theta \leq \frac{1}{2}.$$

After substitution, finite difference representation of the DG method :

$$\frac{d\mathbf{u}_j}{dt} = \frac{1}{\Delta x} (A\mathbf{u}_{j-1} + B\mathbf{u}_j + C\mathbf{u}_{j+1})$$

Fourier stability analysis(von Neumann stability analysis)

Assumption of uniform mesh sizes and periodic boundary conditions:

$$\mathbf{u}_j(t) = \hat{\mathbf{u}}(t)e^{imx_j}, m = 1, 2, 3, \dots$$

Substitute into the matrix form :

$$\frac{d}{dt}\hat{\mathbf{u}}(t) = G\hat{\mathbf{u}}(t)$$

where G is the amplification matrix, given by

$$G = \frac{1}{\Delta x} \left(Be^{-i\xi} + A + Ce^{i\xi} \right), \quad \xi = m\Delta x$$

ODE system from Fourier stability analysis

PDE→ODE→Tools to analyze ODE

If G is diagonalizable, denote the eigenvalues of G as $\lambda_1, \dots, \lambda_{k+1}$ and the corresponding eigenvectors as $\bar{V}_1, \dots, \bar{V}_{k+1}$.

The general solution of the ODE system is

$$\hat{\mathbf{u}}(t) = C_1 e^{\lambda_1 t} \bar{V}_1 + \dots + C_{k+1} e^{\lambda_{k+1} t} \bar{V}_{k+1}$$

where C_1, \dots, C_{k+1} can be determined by the initial condition.

For convenience, write $C_i \bar{V}_i = V_i$

Implement of DG scheme and Fourier analysis when $k=1$

Choose the uniformly spaced points :

$$u_{j-\frac{1}{4}}, u_{j+\frac{1}{4}}, \quad j = 1, \dots, N.$$

Representation of solution through the basis :

$$u(x) = u_{j-\frac{1}{4}}\phi_{j-\frac{1}{4}}(x) + u_{j+\frac{1}{4}}\phi_{j+\frac{1}{4}}(x), \text{ where } \phi_{j\pm\frac{1}{4}}(x) = \begin{cases} 1, & \text{at } \left(j \pm \frac{1}{4}\right) dx \\ 0, & \text{at } \left(j \mp \frac{1}{4}\right) dx \end{cases}.$$

$$\frac{d}{dt} \mathbf{u}_j = \frac{1}{\Delta x} (A \mathbf{u}_{j-1} + B \mathbf{u}_j + C \mathbf{u}_{j+1}) \text{ where } \mathbf{u}_j = \begin{pmatrix} u_{j-\frac{1}{4}}(t) \\ u_{j+\frac{1}{4}}(t) \end{pmatrix}.$$

For simplicity, in this project, we only consider the case for $m = 1$.

Eigenstructure and ODE system when $k=1$

Taylor expansions to eigenvalues:

$$\lambda_1 = -i + \frac{dx^3}{72(2\theta-1)} + \frac{idx^4(6\theta^2-6\theta-1)}{270(1-2\theta)^2} + \frac{dx^5(12\theta^2-12\theta-1)}{648(2\theta-1)^3} + O(dx^6), \theta < 0.5$$

$$\lambda_2 = \frac{6(2\theta-1)}{dx} + 3i + dx(1-2\theta) - \frac{idx^2}{3} + \frac{dx^3(24\theta^2-24\theta+5)}{72(2\theta-1)} + O(dx^4), \theta < 0.5$$

$$\lambda_1 = -i - \frac{idx^2}{48} + \frac{7idx^4}{15360} + \frac{599idx^6}{10321920} + O(dx^8), \theta = 0.5$$

$$\lambda_2 = 3i - \frac{5idx^2}{16} + \frac{83idx^4}{5120} - \frac{313idx^6}{688128} + O(dx^8), \theta = 0.5$$

$$V_1 + V_2 = U_{initial} = \begin{pmatrix} e^{i(-\frac{dx}{4})} \\ e^{i(\frac{dx}{4})} \end{pmatrix}, \quad U_{exact} = e^{-it} \begin{pmatrix} e^{i(-\frac{dx}{4})} \\ e^{i(\frac{dx}{4})} \end{pmatrix}, \quad U_{compute} = e^{\lambda_1 t} V_1 + e^{\lambda_2 t} V_2$$

Observations from eigenvalues when $k=1$

- When $\theta = \frac{1}{2}$, eigenvalues are purely imaginary. The scheme is energy conserving; when $\theta < \frac{1}{2}$, eigenvalues contain a negative real part. The scheme is energy dissipating.
- The error could be decomposed into physical terms and nonphysical terms:

$$\begin{aligned} |u_{\text{exact}} - u_{\text{compute}}| &= |(V_1 + V_2)e^{-it} - e^{\lambda_2 t} b V_2 - e^{\lambda_1 t} V_1| \\ &= |V_2(1 - e^{\lambda_2 t + it}) + V_1(1 - e^{\lambda_1 t + it})| \end{aligned}$$

Physical terms and nonphysical terms have different behavior with time.

Physical terms when $k=1$

The Taylor expansion of physical terms:

$$|V_1(e^{-it} - e^{\lambda_1 t})| = \left(\begin{aligned} &\frac{dx^3 t}{72-144\theta} + \frac{dx^5(2304\theta^4 - 4608\theta^3 + 3936\theta^2 - 1782\theta - 61)t}{129600(1-2\theta)^3} - \frac{dx^6 t^2}{10368(1-2\theta)^2} + O(dx^7) \\ &\frac{dx^3 t}{72-144\theta} + \frac{dx^5(2304\theta^4 - 4608\theta^3 + 3936\theta^2 - 1482\theta - 211)t}{129600(1-2\theta)^3} - \frac{dx^6 t^2}{10368(1-2\theta)^2} + O(dx^7) \end{aligned} \right), \theta \neq \frac{1}{2}$$

$$|V_1(e^{-it} - e^{\lambda_1 t})| = \left(\begin{aligned} &\frac{dx^2 t}{48} - \frac{17dx^4 t}{40960} - \frac{dx^6(t(8960t^2 + 1422369))}{23781703680} + O(dx^7) \\ &\frac{dx^2 t}{48} - \frac{17dx^4 t}{40960} - \frac{dx^6(t(8960t^2 + 1422369))}{23781703680} + O(dx^7) \end{aligned} \right), \theta = \frac{1}{2}$$

- During different time intervals, the dominant terms are different, as observed [7]. For intermediate time, the error is proportional to t . For longer time, another term with higher degree of t may dominate.

This is caused by the expansion of $e^{(\lambda_1+i)t} \approx e^{\frac{dx^3 t}{72(2\theta-1)}}$.

- Bigger θ results in bigger difference between λ_1 and $-i$, thus a bigger error.

Nonphysical terms when $k=1$

λ_2 contains $\frac{1}{dx}$, so $e^{\lambda_2 t}$ could not be directly expanded around $dx=0$.

When $\theta < \frac{1}{2}$, λ_2 would contain a negative real part. $\rightarrow e^{(\lambda_2+i)t}$ would decay exponentially \rightarrow always dropped in the literature [2], [5]. \rightarrow only V_2 is left.

Taylor expansion of V_2 :

$$|-V_2| = \left(\frac{dx^2}{24-48\theta} + \frac{dx^4(-1296\theta^4+2592\theta^3-2056\theta^2+888\theta+83)}{27648(2\theta-1)^3} + O(dx^6) \right), \theta \neq \frac{1}{2}.$$

$$|-V_2| = \left(\frac{dx}{16} - \frac{7dx^3}{1536} + \frac{dx^5}{491520} + \frac{3421dx^7}{660602880} + \frac{8353dx^9}{54358179840} + O(dx^{10}) \right), \theta = \frac{1}{2}.$$

- When θ is bigger, this error would also be bigger.

Nonphysical terms when $k=1$

Based on formula to eigenvalue, when θ is bigger, the real part is bigger, thus $e^{(\lambda_2+i)t}$ would decay more slowly.

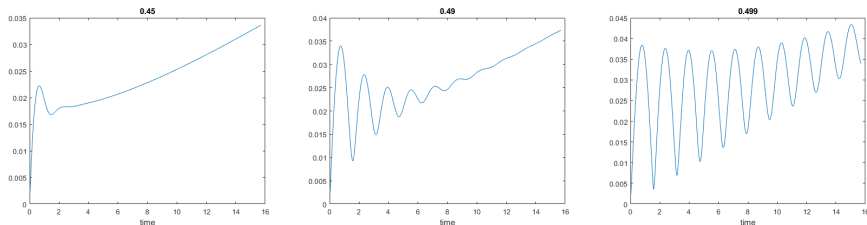


Figure: L-2 Error-time plot. exponential decay. $dx = \frac{\pi}{10}$; $s = 2\pi$; $dt = \frac{dx}{10}$; $t = 5\pi$

Other observations when $k=1$

- Nonphysical terms have stronger influence on short-time error. physical term will dominate in long time simulation.
- Optimal error estimate for energy dissipative scheme and only suboptimal error estimate for energy conservative scheme with central flux. Blow-up behavior caused by $(2\theta - 1)$ in the denominator.
- When θ is smaller, both short time error and long time would be smaller, while the stability region would also be smaller.

Numerical result for different θ when $k=1$

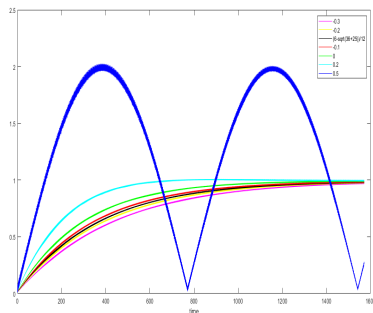


Figure: L^∞ , $dx = \frac{\pi}{5}$, $dt = \frac{dx}{10}$, $t = 500\pi$

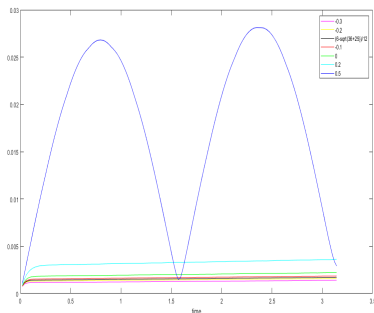


Figure: L^∞ , $dx = \frac{\pi}{10}$, $dt = \frac{dx}{10}$, $t = \pi$

Eigenstructure when k=2

Follow the same procedure, the eigenvalues to G :

$$\begin{pmatrix} \lambda_1 \\ \lambda_2 \\ \lambda_3 \end{pmatrix} = \begin{pmatrix} -i + \frac{dx^5(2\theta-1)}{7200} - \frac{idx^6(14\theta^2-14\theta+1)}{42000} + \frac{dx^7(-48\theta^3+72\theta^2-26\theta+1)}{120000} + O(dx^8) \\ \frac{-i\sqrt{-36\theta^2+36\theta+51+6\theta-3}}{dx} + \frac{84\theta^2 + (-84-14i\sqrt{-36\theta^2+36\theta+51})\theta + 7i\sqrt{-36\theta^2+36\theta+51+1}}{12i\theta^2+2(\sqrt{-36\theta^2+36\theta+51}-6i)\theta - \sqrt{-36\theta^2+36\theta+51}-17i} dx + O(dx^2) \\ \frac{i\sqrt{-36\theta^2+36\theta+51+6\theta-3}}{dx} + \frac{-84\theta^2+14(6-i\sqrt{-36\theta^2+36\theta+51})\theta + 7i\sqrt{-36\theta^2+36\theta+51}-1}{-12i\theta^2+2(\sqrt{-36\theta^2+36\theta+51}+6i)\theta - \sqrt{-36\theta^2+36\theta+51}+17i} dx + O(dx^d) \end{pmatrix}$$

The nonphysical error controls the short time error:

$$V_2 + V_3 = \begin{pmatrix} \frac{idx^3(18\theta+5)e^{-it}}{6480} + \frac{dx^4(1296\theta^2-1728\theta+565)e^{-it}}{388800} + \frac{dx^5e^{-it}(-i(46656\theta^3-85536\theta^2+32994\theta+3875))}{11664000} + O(dx^6) \\ -\frac{1}{240}idx^3(2\theta-1)e^{-it} - \frac{dx^4((432\theta^2-432\theta+23)e^{-it})}{43200} + \frac{dx^5(2\theta-1)e^{-it}(3i(288\theta^2-288\theta+17))}{144000} + O(dx^6) \\ \frac{idx^3(18\theta-23)e^{-it}}{6480} + \frac{dx^4(1296\theta^2-864\theta+133)e^{-it}}{388800} + \frac{dx^5e^{-it}(-i(46656\theta^3-54432\theta^2+1890\theta+2011))}{11664000} + O(dx^6) \end{pmatrix}$$

Major observations when $k=2$

- Similarly, nonphysical terms have stronger influence on short-time error, while the physical term will dominate the error in long time simulation.
- $(2\theta - 1)$ is in the numerator, which would not blow-up when $\theta = \frac{1}{2}$. Hence optimal error estimate for both energy dissipative scheme ($\theta < \frac{1}{2}$) and energy conservative scheme with central flux ($\theta = \frac{1}{2}$).
- On the contrary, when θ is bigger, both short time error and long time would be smaller.

Numerical result for different θ for long time, $k=2$

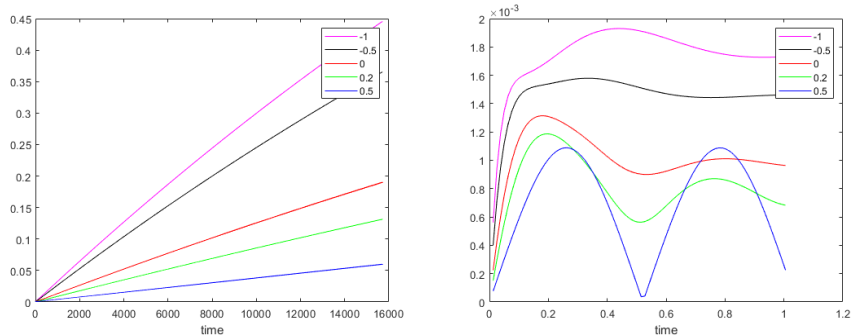
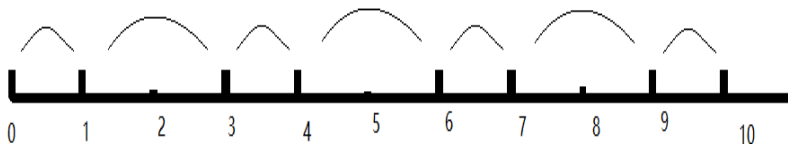


Figure: L^∞ error; $dx = \frac{\pi}{5}$, $dt = \frac{dt}{10}$, long time : 5000π , short time = 1

"Nonuniform" mesh

Here the Quasi-uniform mesh region is specially constructed by two different mesh sizes. $\Delta x_{\text{left}} / \Delta x_{\text{right}} = 2$.



It reveals some property toward the nonuniform mesh.

Physical eigenvalue on nonuniform mesh

When $k=1$, physical eigenvalue :

$$-i + \frac{dx^3}{432} \left(9(2\theta - 1) + \frac{25}{2\theta - 1} \right) - \frac{idx^4 (90\theta^4 - 180\theta^3 + 94\theta^2 - 4\theta + 11)}{270(1 - 2\theta)^2} + O(dx^5), \theta \neq \frac{1}{2}$$

When $k=2$, physical eigenvalue :

$$-i + \frac{dx^5}{43200} (81(2\theta - 1) + \frac{49}{2\theta - 1}) - \frac{idx^6 (1134\theta^4 - 2268\theta^3 + 1418\theta^2 - 284\theta + 43)}{42000(1 - 2\theta)^2} + O(dx^7)$$

- $(1-2\theta)$ occur in both numerator and denominator
→ $\theta = \frac{1}{2}$ would blow-up
→ suboptimal error estimate.

Convergence order on nonuniform mesh

number of cells(3dx long)	order, $k=2, \theta = 0.5$	order, $k=2, \theta = 0$	order, $k=1, \theta = 0.5$	order, $k=1, \theta = 0$
50(50 * 2 * 2 points)				
100, $t=1$	2.1263	2.9239	0.9909	1.9995
200	2.1350	2.9623	0.9954	1.9996
400	2.0803	2.9748	0.9976	1.9996
600	2.0696	2.9789	0.9978	1.9997
800	2.0610	2.9811	0.9980	1.9997
1000	2.0576	2.9825	0.9983	1.9997

Table: convergence order on nonuniform mesh, $k=2$

- When $k=1$, convergence order is the same as on uniform mesh.
- When $k=2$ and $\theta = \frac{1}{2}$, convergence order would be suboptimal (second order) on nonuniform mesh.
Recall on uniform mesh it remains optimal error estimate(third order).
Proved theoretically by projection operator in [6].

Relationship between error and θ on nonuniform mesh

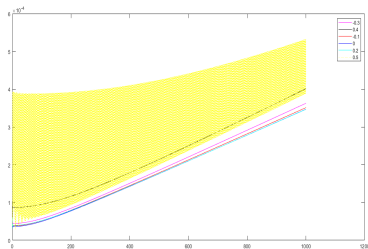
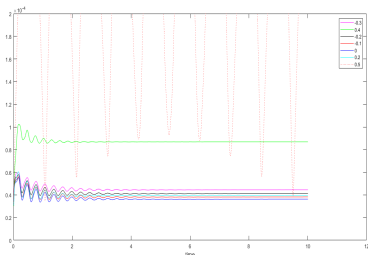


Figure: l^2 error for different θ on nonuniform mesh, $k=2,3, dx = \frac{\pi}{10}, dt = \frac{dt}{10}$

- The error is not monotone with θ on nonuniform mesh.
- Same behavior is observed for $k=1$.
- Long time error behavior could be explained by eigenvalue.

Summary of results on nonuniform mesh

Comparing the results on uniform mesh and nonuniform mesh:

	upwind biase,k=1	upwind biase,k=2	central flux,k=1	central flux,k=2
uniform mesh	2	3	1	3
nonuniform mesh	2	3	1	2
error when θ increases	increase	decrease	indeterminate	indeterminate

Table: L2 error, order of accuracy and relationship between θ and error

Brief introduction to Fu's method

A new optimal, energy-conserving DG methods proposed in [4].

Double the unknowns and equations by introducing an auxiliary zero function

$$\begin{aligned} u_t + cu_x &= 0, (x, t) \in I \times (0, T], \\ \phi_t - c\phi_x &= 0, (x, t) \in I \times (0, T], \end{aligned} \quad u(x, 0) = u_0(x), \phi(x, 0) = 0$$

The flux used here : by

$$\hat{u}_h|_{j-\frac{1}{2}} = \{u_h\}|_{j-\frac{1}{2}} + \frac{1}{2}\alpha[\phi_h]\Big|_{j-\frac{1}{2}}, \quad \hat{\phi}_h|_{j-\frac{1}{2}} = \{\phi_h\}|_{j-\frac{1}{2}} + \frac{1}{2}\alpha[u_h]\Big|_{j-\frac{1}{2}}, \alpha \in R$$

Follow the same procedure to get the amplification matrix G.
The expansion of eigenvalues

$$\begin{aligned}\lambda_1 &= -i + \frac{i(6a^2-5)dx^4}{1080a^2} + \frac{i(144a^4-357a^2+224)dx^6}{217728a^4} + O(dx^8) \\ \lambda_2 &= i - \frac{i(6-\frac{5}{a^2})dx^4}{1080} - \frac{i(144a^4-357a^2+224)dx^6}{217728a^4} + O(dx^8) \\ \lambda_3 &= \frac{6ia}{dx} + \left(\frac{3i}{4a} - ia\right)dx + \frac{i(48a^4-16a^2-27)dx^3}{576a^3} - \frac{i(576a^6-432a^4+1060a^2-1215)dx^5}{207360a^5} + O(dx^6) \\ \lambda_4 &= -\frac{6ia}{dx} + \left(ia - \frac{3i}{4a}\right)dx - \frac{i(48a^4-16a^2-27)dx^3}{576a^3} + \frac{i(576a^6-432a^4+1060a^2-1215)dx^5}{207360a^5} + O(dx^6)\end{aligned}$$

The numerical solution :

$$\begin{pmatrix} \hat{u}_{m,-\frac{1}{4}}(t) \\ \hat{u}_{m,\frac{1}{4}}(t) \\ \hat{\phi}_{m,-\frac{1}{4}}(t) \\ \hat{\phi}_{m,\frac{1}{4}}(t) \end{pmatrix} = e^{\lambda_1 t} V_1 + e^{\lambda_2 t} V_2 + e^{\lambda_3 t} V_3 + e^{\lambda_4 t} V_4.$$

Results from Fourier Analysis

- Eigenvalues are all purely imaginary \rightarrow Scheme is energy conserving.
- When $\alpha = \sqrt{\frac{5}{6}}$, the physical eigenvalue would be closest to exact eigenvalue. Phase difference and long time error would be smaller. Consistent with the result in [1].
- α occurs in the denominator of eigenvalue. When $\alpha=0$, the scheme would blow and be suboptimal. Note that when $\alpha = 0$, the scheme is the same as central flux scheme.

Prediction by phase difference

In [1], it is observed different scheme could have similar phase error at different time.

physical eigenvalue \rightarrow phase difference \rightarrow shape of numerical solution

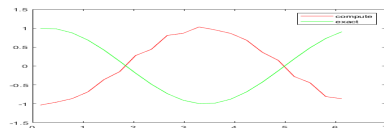
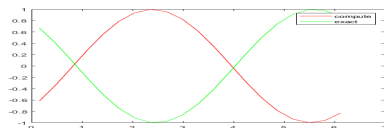


Figure: $dx = \frac{1}{5}\pi$; $s = 2\pi$; $dt = \frac{dx}{20}$. Fu's method at $t=21769$; central flux at $t=382$

Conclusion and future work

Conclusions

- We decomposed the error into physical and nonphysical components and discussed their different behavior with time.
- We explore the relationship between error and θ for the upwind biased DG scheme.
- We verified a few existing convergence results with the Fourier approach for the upwind biased DG scheme, the DG scheme with central flux, and the energy-conserving scheme in [4].

Ongoing and future work

- Relation ship between blow-up behavior caused by the parameter in denominator and suboptimal error estimate.
- The symbolic results which could hardly be computed now due to limited computation power.
- Superconvergence result through Fourier analysis.

Reference



Mark Ainsworth and Guosheng Fu.

Dispersive behavior of an energy-conserving discontinuous galerkin method for the one-way wave equation.
Journal of Scientific Computing, 79(1):209–226, 2019.



Nattaporn Chuenjarern and Yang Yang.

Fourier analysis of local discontinuous galerkin methods for linear parabolic equations on overlapping meshes.
Journal of Scientific Computing, 81(2):671–688, 2019.



Daniel J Freaun and Jennifer K Ryan.

Superconvergence and the numerical flux: a study using the upwind-biased flux in discontinuous galerkin methods.
Communications on Applied Mathematics and Computation, pages 1–26, 2019.



Guosheng Fu and Chi-Wang Shu.

Optimal energy-conserving discontinuous galerkin methods for linear symmetric hyperbolic systems.
Journal of Computational Physics, 394:329–363, 2019.



Wei Guo, Xinghui Zhong, and Jing-Mei Qiu.

Superconvergence of discontinuous galerkin and local discontinuous galerkin methods: eigen-structure analysis based on fourier approach.
Journal of Computational Physics, 235:458–485, 2013.



Yong Liu, Chi-Wang Shu, and Mengping Zhang.

Sub-optimal convergence of discontinuous galerkin methods with central fluxes for even degree polynomial approximations.
arXiv preprint arXiv:2001.03825, 2020.



Xinghui Zhong and Chi-Wang Shu.

Numerical resolution of discontinuous galerkin methods for time dependent wave equations.
Computer Methods in Applied Mechanics and Engineering, 200(41-44):2814–2827, 2011.